

Analytical Tension Stiffening Model for Concrete Beam Reinforced with Inoxydable Steel

Sophia C. Alih^{1*}, Abdelouahab Khelil², Mohammadreza Vafaei³ and Nur Hajarul Falahi Abd Halim⁴

¹Faculty of Civil Engineering, Institute of Noise and Vibration, Universiti Teknologi, Malaysia.
 Orcid: 0000-0001-5326-3670

²Université de Lorraine, IJL UMR 7198 CNRS – Equipe 207, Villers Les Nancy, France.
 Orcid: 0000-0001-9707-170X

³Faculty of Civil Engineering, Forensic Engineering Center, Universiti Teknologi, Malaysia.
 Orcid: 0000-0002-9988-1842

⁴Faculty of Civil Engineering, Universiti Teknologi, Malaysia.
 Orcid: 0000-0003-0527-7722

*Corresponding Author

Abstract

Unlike the conventional carbon steel that has been used widely as reinforcement bars, the usage of Inoxydable steel (Inox) is still limited despite their superior properties in strength and ductility. Hence, limited study has been conducted to determine the structural behavior of Inox including the constitutive law and material model when it is used as reinforcement bars in concrete element. In this study, tension stiffening model is specifically developed for Inox to determine their interaction properties with the surrounding concrete. This study uses constitutive laws developed for Inox from Austenitic type. An inverse method based on combination of results from experimental works and the one obtained from nonlinear numerical analysis (NNA) is applied to determine the parameters involved in the tension stiffening model. The tension stiffening model developed for inoxydable steel is then compared with the conventional carbon steel. Results from this study shows that the inverse method is able to develop tension stiffening model for concrete beam reinforced with inoxydable steel. When compared with carbon steel, tension stiffening for inoxydable steel is 50 percent higher during the cracking phase. Findings from this study; tension stiffening model parameters for inoxydable steel are very useful for modeling works which uses Inox as reinforcing steel bars.

Keywords: Inoxydable steel, Tension-stiffening model, Reinforced concrete beam, Section analysis, Nonlinear numerical analysis

INTRODUCTION

In reinforced concrete structures, the presence of steel necessitates the consideration of bar-concrete interaction. The bar-concrete adherence allows the concrete located between

cracks to resist tensile stresses, thereby reducing the average reinforcement stress level compared to its magnitude at the crack. This phenomenon results in a gain in rigidity, called tension stiffening [1].

A simple way to account for this local phenomenon is to integrate the bar-concrete interaction in a global dimension by modifying the stress-strain relationship of the material, either the reinforcing bar or the concrete [2]. Several investigators have developed the tension stiffening model by modifying the concrete material model. After reviewing different model developed by other researchers, tension stiffening model proposed by [3] shown in Figure 1 is chosen to represent the interaction properties between Inox and concrete. It depicts the main phenomena of primary and secondary stage. Four parameters; C_d , C_b , C_p , and C_s are used to define the entire model together with concrete properties of f'_t and ϵ_{cr} ;

$$f'_t = 0.3f_{ck} \left(\frac{2}{3}\right)$$

$$\epsilon_{cr} = \frac{f'_t}{E}$$

where, f_{ck} is compressive strength of concrete, and E is the modulus of elasticity

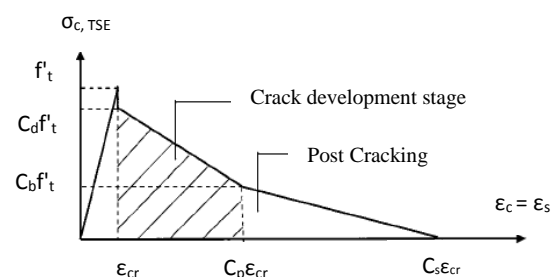


Figure 1: Tension stiffening model used in the study

The tension stiffening model is one of important parameter to consider in any numerical modeling involving reinforced concrete composite. Since this model represents the interaction behavior between concrete and reinforcing bars in the model, accurate parameters which represent the type of reinforcing bars used are crucial in order to have a model closely represents the actual condition of the reinforced concrete structure. Tension stiffening model to represent interaction properties between carbon steel and the surrounding concrete has been developed by other researchers. Despite their excellence resistance to corrosion, superior strength, and high ductility which gives it the potential application as reinforcement bars [4-6], studies involving this type of reinforcement bars are still limited [7]. Based on the authors' knowledge, tension stiffening model which determines interaction properties between Inox and concrete has not yet been developed.

Therefore, this study aims to develop a set of tension stiffening parameters that resemble the interaction properties between inoxydable steel and concrete. This model is then compared with the one with standard carbon steel as reinforcing bars. Constitutive law used to represent the behavior of inoxydable steel used in this study is developed based on series of laboratory works [8] and therefore valid to be used in other numerical model involving this type of steel. Furthermore, the approach used in this study has been demonstrated to be able to determine the interaction properties through bending test instead of direct tension as been reported by other researchers [9-13].

METHOD AND APPROACH

In order to determine the four parameters in the tension stiffening model, NNA is conducted on the beam section to determine the load-deflection curve based on the section and beam properties. This analysis consist of two main stages; i) section analysis, ii) beam analysis. Figure 2 shows the steps taken during the NNA. In the beginning of the analysis, initial values of the tension stiffening parameters are introduced to the program together with the other properties of the RC beam obtained from laboratory samples. These include the materials and geometrical properties.

In the first iteration, section analysis is conducted followed by beam analysis. Section analysis will provide the properties detail for a particular section of the beam for each load increment. These properties will then be used in the beam analysis in order to determine load-deflection curve at mid-span of the beam. The load-deflection curve obtained from this NNA is then compared with the one obtained from laboratory work; bending test on the beam sample. The tension stiffening model applied in the section analysis is then corrected by changing the values of the four parameters; C_d , C_b , C_p , C_s so the load-deflection curve values from NNA resemble well with the laboratory results. The set of parameters which give the best-fit values with laboratory is selected as the tension stiffening model to represent the concrete beam reinforced with Inoxydable steel bars. These inversely estimated values give more reliable representation of interaction properties between the Inox and composite concrete.

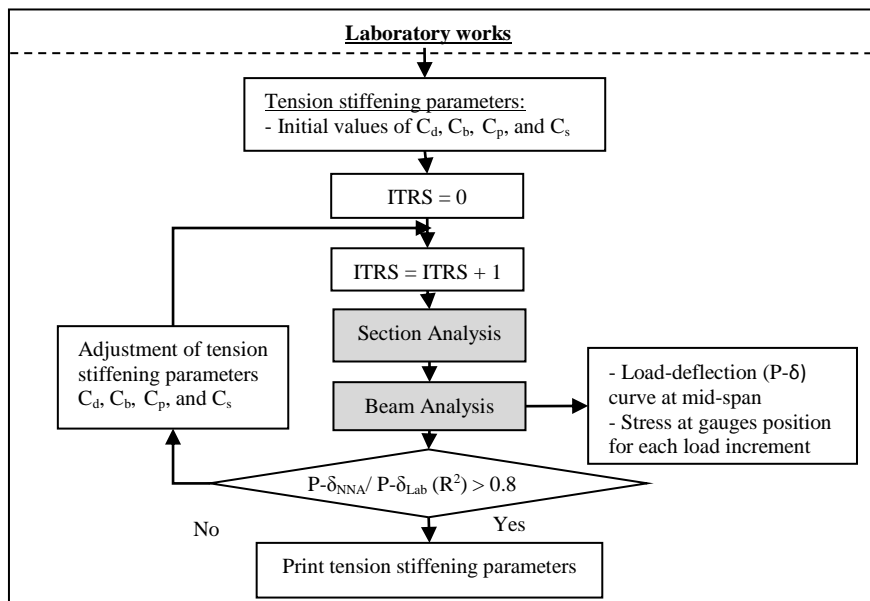


Figure 2: Steps in the nonlinear numerical analysis

If the coefficient of determination, R^2 between the two curves is more than 0.8, the values set of C_d , C_b , C_p , C_s will be chosen

as the tension stiffening parameters for Inoxydable steel. Otherwise, second iteration will be conducted with a new set

of parameters and the whole process will be repeated all over again.

Section Analysis

Increasing the loading (axial force and/or bending moment) applied to a section, causes the neutral axis depth, the strain and stress distributions, and the flexural and axial rigidities to vary in a nonlinear manner. Numbers of studies involving numerical techniques have therefore been conducted to tackle this situation. Bilinear and trilinear moment-curvature relations for flexural members are example of early and simple models. However, such models are incapable of tracing an accurate response for heavily reinforced sections, especially in presence of an axial force [3]. In this study, a nonlinear solution scheme is utilized within which direct and exact computations are made by performing closed-form integrations for nonlinear section properties. The section analysis involved determination of overall effective or secant flexural rigidity (EIs) for the beam section. The strain profile is determined using the applied moment and the current value of the EIs about the inelastic centroid. The compression and tension zones of the section are identified.

Material Models:

a) *Concrete behavior in compression*

For concrete layers in compression zones, a fourth-degree polynomial model is chosen to represent the stress-strain relation [14];

$$\sigma_c = a_0 + a_1 \varepsilon_c + a_2 \varepsilon_c^2 + a_3 \varepsilon_c^3 + a_4 \varepsilon_c^4 \quad [1]$$

The above polynomials have been proposed on the basis of agreement with experimental work. The coefficients in Eq. [1] are defined by using the curve boundary condition based on concrete properties;

$$\begin{Bmatrix} a_0 \\ a_1 \\ a_2 \\ a_3 \\ a_4 \end{Bmatrix} = \begin{bmatrix} 1 & 0 & 0 & 0 & 0 \\ 0 & 1 & 0 & 0 & 0 \\ 1 & \varepsilon_m & \varepsilon_m^2 & \varepsilon_m^3 & \varepsilon_m^4 \\ 0 & 1 & 2\varepsilon_m & 3\varepsilon_m^2 & 4\varepsilon_m^3 \\ 1 & 1 & 2C_u\varepsilon_m & 3(C_u\varepsilon_m)^2 & 4(C_u\varepsilon_m)^3 \end{bmatrix}^{-1} \begin{Bmatrix} 0 \\ E_{ci} \\ f_m \\ 0 \\ E_{cf} \end{Bmatrix} \quad [2]$$

where, $f_m = k_c \cdot f'_c$, $k_c = 0.85, 1.0$ or > 1.0 according to some investigators. In this study k_c is taken as 1.0. E_{ci} is the initial modulus of elasticity, E_{cf} is the modulus of elasticity at the ultimate strain, C_u taken as 1.5 and ε_m is the maximum strain.

b) *Concrete behavior in tension*

The stress-strain relation of reinforced concrete shown in Figure 1 is used to represent the tensile behavior of the RC beam. This relation is well backed by experimental curve of

plain concrete and compared well with test results by other researchers. Furthermore it is well suited to the present method of analysis. The four parameters C_d, C_b, C_p, C_s are set to an initial trial values at the beginning of the analysis and inversely estimated from a combination of nonlinear analysis and experimental results.

c) *Stress-strain relation for reinforcing steel*

A bilinear relation is considered adequate for proper simulation of the actual stress-strain relation for reinforcing steel used in compression zone (carbon steel Grade 460) since the elastic-plastic behavior with or without introducing the strain hardening effect is easily simulated by controlling the slope of the second line. However, for tension zone where Inoxydable steel bars are used, a specific constitutive law developed in a previous study conducted by the authors [8]; Eq. [3] and [4] are applied to represent the nonlinearity of this type of steel.

$$\varepsilon = \frac{\sigma}{177\,305} + 0.002 \left(\frac{\sigma}{480}\right)^{5.56} \quad \text{for } \sigma \leq \sigma_{0.2} \quad [3]$$

$$\varepsilon = \frac{\sigma - 480}{34\,724} + 0.38 \left(\frac{\sigma - 480}{293}\right)^{3.17} + 0.0047 \quad \text{for } \sigma > \sigma_{0.2} \quad [4]$$

where $\sigma_{0.2}$ is the stress at 0.2% proof stress; taken as limit of elasticity for the inox.

Terminology and Basic Concept :

Considering the axial rigidity (EA_s) as the overall effective elasticity modulus of the section times its area, the integrated form of EA is given by:

$$EA_s = \int_{Y_N}^{H+Y_N} E(Y) \cdot B \cdot dY + \sum_{i=1}^N (E_{sti} - E_{cti}) A_{sti} + \sum_{j=1}^M (E_{sbj} - E_{cbj}) A_{sbj} \quad [5]$$

$$E(Y) = \frac{\sigma(Y)}{\varepsilon(Y)} \quad [6]$$

$$E_{sti} = \frac{\sigma_{sti}}{\varepsilon_{sti}} \quad [7]$$

$$E_{sbj} = \frac{\sigma_{sbj}}{\varepsilon_{sbj}} \quad [8]$$

where N, M are the numbers of the top and bottom reinforcement layers, respectively.

The flexural rigidity (EI_s) is the overall effective elasticity

modulus of the section times the moment of inertia about the inelastic centroid (Y_c), the inelastic centroid being the position about which the first moment of the axial rigidity (EA) vanishes; Figure [5(a)]. Hence

$$EI_s = \int_{Y_N}^{H+Y_N} E(Y).B.(Y - Y_o)^2 .dY + \sum_{i=1}^N (E_{sti} - E_{cti}) A_{sti} (H + Y_N - Y_{sti} - Y_o)^2 + \sum_{j=1}^M (E_{sbj} - E_{cbj}) A_{sbj} (Y_N - Y_{sbj} - Y_o)^2 \quad [9]$$

The curvature of the section (ϕ) is obtained, as usual, by dividing the moment (M_o) about the inelastic centroid by the flexural rigidity (EI_s). The internal axial force is given by:

$$F_x = \int_{Y_N}^{H+Y_N} \sigma(Y).B.dY + \sum_{i=1}^N (E_{sti} - E_{cti}) \varepsilon_{sti} A_{sti} + \sum_{j=1}^M (E_{sbj} - E_{cbj}) \varepsilon_{sbj} A_{sbj} \quad [10]$$

The internal bending moment (M_{int}) about the inelastic centroid is represented by:

$$M_{int} = \int_{Y_N}^{H+Y_N} \sigma(Y).B.(Y - Y_o)^2 .dY + \sum_{i=1}^N (E_{sti} - E_{cti}) \varepsilon_{sti} A_{sti} (H + Y_N - Y_{sti} - Y_o) + \sum_{j=1}^M (E_{sbj} - E_{cbj}) \varepsilon_{sbj} A_{sbj} (Y_N - Y_{sbj} - Y_o) \quad [11]$$

Analytical Procedures:

To develop an approach which lends itself to direct computation, the section is divided into two zones each of which is bounded by one of the extreme fibers and the neutral axis. According to the type of stress in any zone (tension or compression), it is further divided into regions having a certain stress-strain formula for each. The compression zone may include one or more of the following regions (Referring to Figure 3 for concrete region):

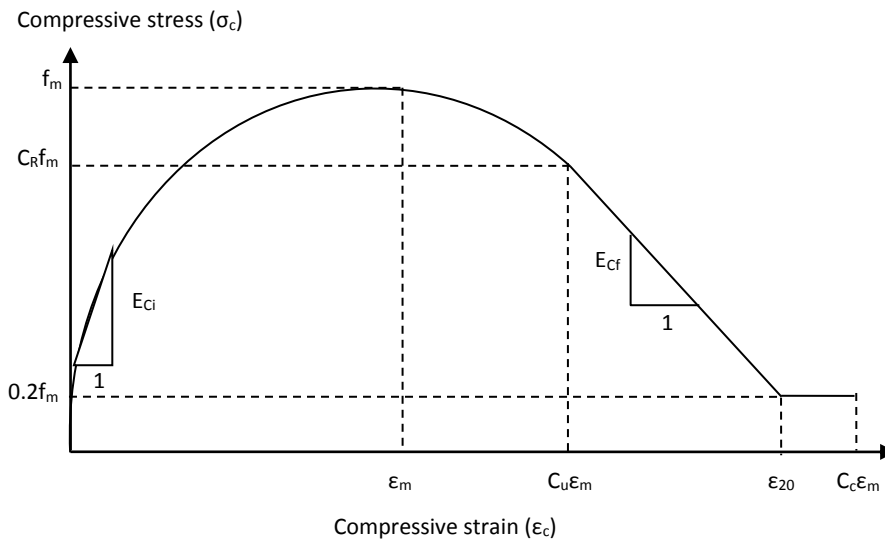


Figure 3: Stress-strain relationship for concrete in compressive zone

Concrete:

Region 1: $0 \leq \varepsilon_c \leq C_u \varepsilon_m$

Steel: Region 4: $0 \leq \varepsilon_{sc} \leq \varepsilon_y$

Region 2: $C_u \varepsilon_m < \varepsilon_c \leq \varepsilon_{20}$

Region 5: $\varepsilon_y \leq \varepsilon_{sc} \leq \varepsilon_{su}$

Region 3: $\varepsilon_{20} < \varepsilon_c \leq C_c \varepsilon_m$

For steel, ε_y = yield strain, ε_{su} = ultimate strain

The tension zone may also include one or more of the

following regions (Referring to Figure 1 for concrete region):

Concrete: Region 1: $-\varepsilon_{cr} \leq \varepsilon_t \leq 0$

Steel: Region 4: $-\varepsilon_y \leq \varepsilon_{st} \leq 0$

Region 2: $-C_p \varepsilon_{cr} \leq \varepsilon_t \leq -\varepsilon_{cr}$

Region 5: $-\varepsilon_{su} \leq \varepsilon_{st} \leq -\varepsilon_y$

Region 3: $-C_s \varepsilon_{cr} \leq \varepsilon_t \leq -C_p \varepsilon_{cr}$

Explicit forms of the rigidities and the internal loadings for all the regions are derived by performing analytical integrations. By the summation of the region properties, the section

properties are directly obtained.

$$EA_s = \sum_{i=1}^2 \sum_{j=1}^{NRi} EA_{ij} \quad [12]$$

$$F_x = \sum_{i=1}^2 \sum_{j=1}^{NRi} F_{xij} \quad [13]$$

$$EI_s = \sum_{i=1}^2 \sum_{j=1}^{NRi} EI_{ij} \quad [14]$$

$$M_{int} = \sum_{i=1}^2 \sum_{j=1}^{NRi} M_{cij} \quad [15]$$

where NRi is the number of regions per zone.

The effective section properties corresponding to any applied bending moment step, M , are evaluated as follows. The procedures are programmed in MATLAB and simplified in the flowchart shown in Figure 4.

1. The instantaneous curvature is determined by dividing the applied moment by the most current value of the effective section flexural rigidity:

$$\phi = \frac{M}{EI_s} \quad [16]$$

2. The depth of the tension and the compression zones are

defined using the most recent location of the inelastic centroid Y_c and the total height of the section H : $Y_{N1} = H - Y_c$ and $Y_{N2} = Y_c$

3. The section rigidities (EA_s , EI_s), internal axial force (F_x), and the bending moment (M_{int}) are calculated for the present strain distribution using Eqs. [12] – [15].
4. The accuracy of the most recent inelastic centroid position is investigated using the criterion of vanishing the moment of axial rigidity about the current centroid (ES) at the correct position:

$$ES = \frac{F_x}{\phi} \quad [17]$$

A normalized convergence criterion is adopted with a certain tolerance limit depending on the level of accuracy desired. The tolerance used in this study is 5×10^{-7} :

$$\frac{ES}{EA_s x Y_c} \leq Tolerance \Rightarrow Convergence \text{ achieved} \quad [18]$$

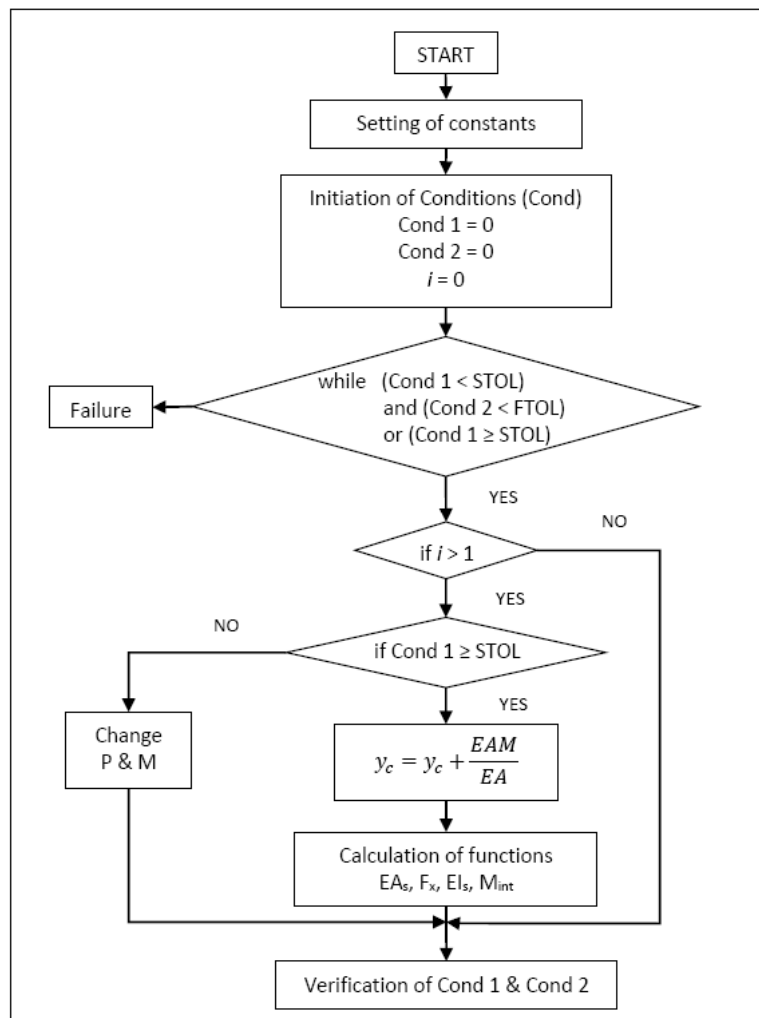


Figure 4: Flow chart of the nonlinear numerical analysis programmed using MATLAB

5. If Eq. [18] is satisfied, an equilibrium solution is reached, yielding the inelastic centroid position and the section properties for that step. Otherwise, steps 1-4 are repeated using the corrected inelastic centroid Y_c until convergence is achieved:

$$Y_{c(\text{corrected})} = Y_{c(\text{current})} + \frac{ES}{EA_s} \quad [19]$$

6. The analysis is stopped when a failure criterion is satisfied. The failure criteria implemented are rupture of reinforcement or crushing of concrete. Concrete crushing failure is defined at 0.003 compressive strain for unconfined compression and a higher value for confined concrete (the strain at which the compression stress of the descending branch reaches $0.2 f_c$). Rupture failure occurs when the reinforcement reaches the ultimate rupture strain.

Beam Analysis

The nonlinear load-deflection solution of the beam is formulated using the moment area integration. Because the flexural rigidity reduces with an increase in moment, the stiffness of the beam is expected to vary along the span, in a nonlinear fashion, with the change in bending moment. This study is intended to consider an accurate stiffness distribution along the beam. This is accomplished by dividing the beam into a large number of segments and calculating the section flexural rigidity in the middle of each segment under a certain

load increment. The mid-span deflection, in symmetrically loaded simple beams, is obtained by performing numerical integration of the moment of curvature distribution along half the span about the support point. The numerical integration is performed as a summation of the analytical integration contribution of each segment. This is expressed for the four-point bending case as

$$\Delta_{\text{midspan}} = \int_0^{L/2} x\varphi(x)dx = \sum_{i=1}^{N_s} \frac{P}{2EI_{si}} \left[\frac{X_{i+0.5}^3 - X_{i-0.5}^3}{3} \right] + \frac{PL_a}{2EI_{si}} \left[\left(\frac{L}{2} \right)^2 - (L_a)^2 \right] \quad [20]$$

where N_s =number of segments along the beam shear span; P =total load applied on the beam; $X_{i-0.5}$ =distance from the support point to the beginning of segment i ; $X_{i+0.5}$ =distance from the support point to the end of the segment i ; L_a =shear span of the beam, and EI_{si} =flexural rigidity of segment i .

The mid-span deflection is then plotted and compared to the curve obtained from laboratory test, as shown in Figure [5(b)]. The tension stiffening model applied in the section analysis is then corrected by changing the values of the four parameters; C_d , C_b , C_p , C_s so the load-deflection curve values from NNA resemble well with the laboratory results. The set of parameters which give the best-fit values with laboratory is selected as the tension stiffening model to represent the concrete beam reinforced with Inoxydable steel bars. These inversely estimated values give more reliable representation of interaction properties between the Inoxy and composite concrete.

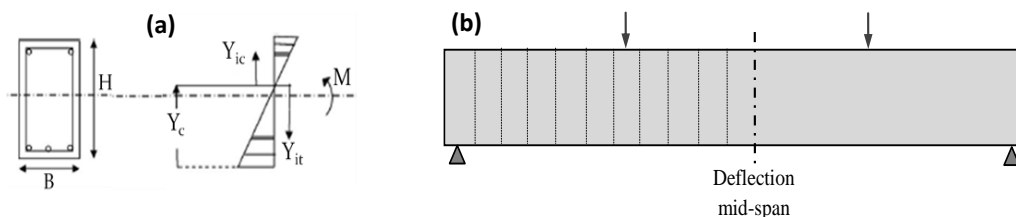


Figure 5: (a) Basic parameters used for analyzing RC sections, (b) Beam is divided into a large number of sections to determine the central deflection for every increment of load

RESULTS AND ANALYSIS

Results obtained from the NNA are compared with laboratory findings in order to determine the tension stiffening model for Inoxy. A beam sample is constructed and tested under bending. Results are used as input to the nonlinear numerical analysis.

Preparation and testing of beam sample

Fig. 6 shows the dimension of the reinforced concrete beam sample used in this study. A 2.95m long simply supported beam subjected to four point bending is used. This composite

concrete beam is reinforced with two bars (20mm diameter) of inoxydable steel from austenitic type in the tension zone, and two bars (8mm diameter) of carbon steel in the compression zone. 10 shear links formed from 6mm mild steel bars were provided at 70mm and 120mm from each ends for shear reinforcement in the shear spans. The beam were tested on simply supported condition with a clear span of 2.9m and loaded symmetrically and monotonically. Crushing test on the concrete sample in accordance with [15] were conducted to identify the compressive strength of the concrete; $f_c = 50$ MPa, and the Young's Modulus of the concrete is 37,565 MPa.

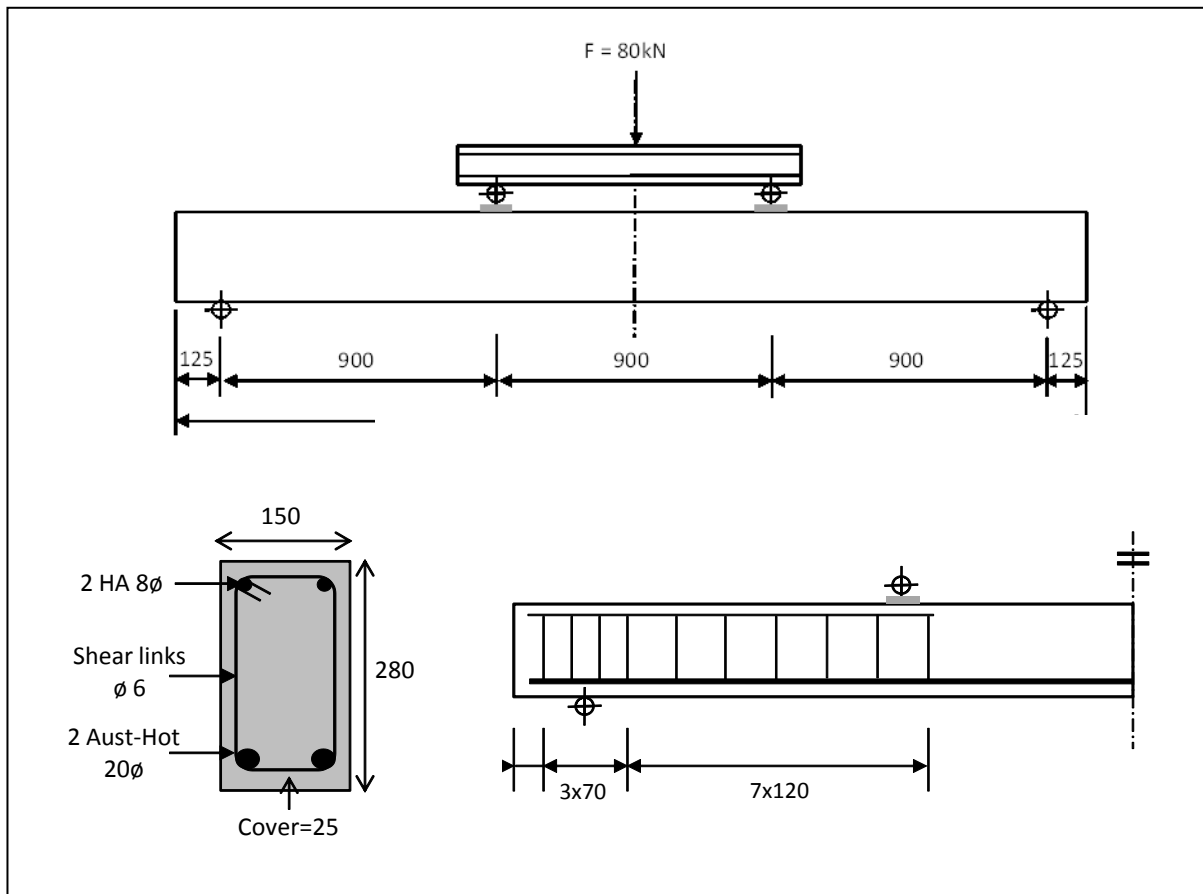


Figure 6: Dimension of the RC beam as per constructed and tested in laboratory (units are in millimeter)

125

Determination of Tension Stiffening Parameters

A series of analyses are conducted to determine the tension stiffening parameters that correlate well with the real behavior of the RC beam as per laboratory findings. Table 1 shows the four sets of trial on selecting the values of C_d , C_b , C_p , C_s . Based on the section properties obtained from NNA, and load-deflection values from beam analysis, comparison with laboratory results gives value of 0.9, 0.6, 4 and 40 for C_d , C_b , C_p , C_s respectively. The load-deflection curve from NNA using these tension stiffening parameters are compared with laboratory curve in Figure 7. Good correlation can be observed from these two curves. Figure 8 shows the final tension stiffening model develop for composite concrete beam reinforced with inoxydable steel from austenitic type. This model is useful to represent the interaction behavior between these two materials in any finite element modeling works.

Table 1: Investigation of tension stiffening parameters

Parameter	Selecting C_d	Selecting C_b	Selecting C_p	Selecting C_s	Selected parameters
C_d	0.8, 0.9 , 1	1.5	1.5	1.5	0.9
C_b	0.5	0.45, 0.5 , 1	0.8	0.8	0.5
C_p	4	4	4, 5 , 6	4	5
C_s	40	40	40	5, 10, 13 , 20	13

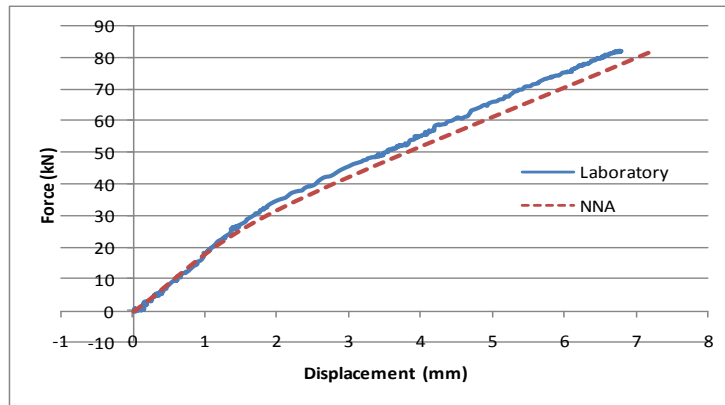


Figure 7: Force displacement curve from laboratory results compared to the nonlinear numerical analysis

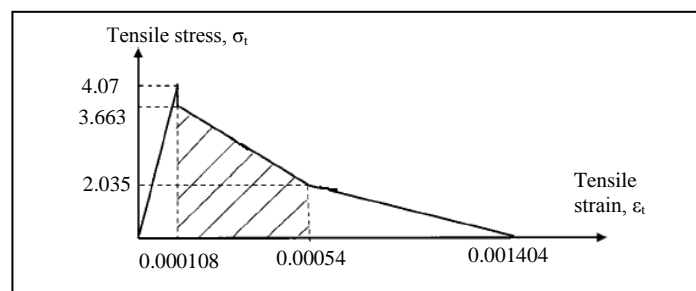


Figure 8: Tension stiffening model for beam reinforced with inoxydable steel bars

Comparison with Carbon Steel

According to a study conducted by [3], selected values for tension stiffening parameters for concrete beam reinforced with carbon steel are 0.8, 0.45, 4, and 10 for C_d , C_b , C_p , and C_s respectively. Figure 9 shows the tension stiffening model for inoxydable steel as compared to the standard carbon steel.

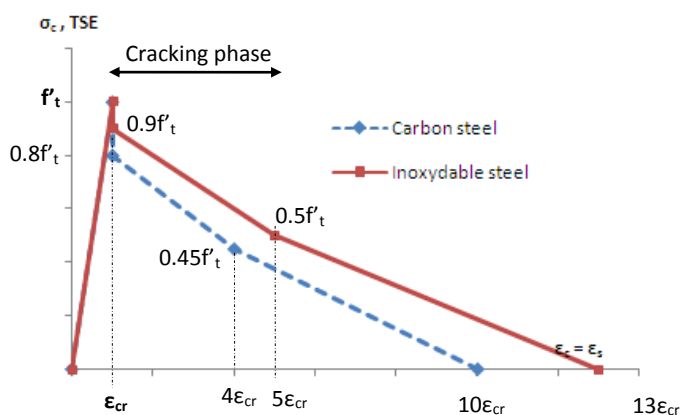


Figure 9: Comparison of tension stiffening model for concrete beam reinforced with carbon steel and inoxydable steel

Referring to Figure 9, it can be observed that concrete beam reinforced with inoxydable steel has higher tension stiffening effect than the one reinforced with standard carbon steel. In

the cracking phase, the tension stiffening with inoxydable steel increases 50 percent as compared to standard steel.

CONCLUSIONS

Approach suggested in this study is able to determine parameters involved in developing the tension stiffening model through combination of numerical modeling and experimental results. Results from bending test can be used instead of direct tension which required more experimental set up. This tension stiffening model could be used further in any numerical simulation to represent the interaction properties between inoxydable steel and concrete in composite material. Findings from this study increases the understanding on the behavior of Inoxydable steel when it is used as reinforcement bars in concrete element.

ACKNOWLEDGEMENT

The authors would like to acknowledge supports from Universiti Teknologi Malaysia, Université de Lorraine, and the financial support from Ministry of Higher Education of Malaysia through the Fundamental Research Grant Scheme (4F292 and 4F716).

REFERENCES

- [1] Yuichi Sato and Frank J. Vecchio, Tension stiffening and crack formation in reinforced concrete members with fiber-reinforced polymer sheets, *Journal of Structural Engineering* 2003; 129 (6): 717-724.
- [2] Ying-Wu Zhou and Yu-Fei Wu, General model for constitutive relationships of concrete and its composite structures, *Composite Structures* 2011; 08(022): 1-13.
- [3] Rim Nayal and Hayder A. Rasheed, Tension stiffening model for concrete beams reinforced with steel and FRP bars, *Journal of Materials in Civil Engineering* 2006; 18(6): 831-841.
- [4] A. Bautista, G. Blanco, F. Velasco, M.A. Martinez, Corrosion performance of welded stainless steels reinforcements in simulated pore solutions, *Construction and Building Materials* 2007; 21: 1267–1276.
- [5] A. Bouchaïr, J. Averseng, A. Abidelah, Analysis of the behavior of stainless steel bolted connections, *Journal of Constructional Steel Research* 2008; 7(9): 1-11.
- [6] Goitseone Malumbela, Mark Alexander, Pilate Moyo, Variation of steel loss and its effect on the ultimate flexural capacity of RC beams corroded and repaired under load, *Construction and Building Materials* 2010; 24: 1051–1059.
- [7] F. Velasco , G. Blanco, A. Bautista, M.A. Martínez, Effect of welding on local mechanical properties of stainless steels for concrete structures using universal hardness tests, *Construction and Building Materials* 2009; 23: 1883–1891.
- [8] S. Alih, A. Khelil, Behavior of Inoxydable Steel and their Performance as Reinforcement Bars in Concrete Beam: Experimental and Nonlinear Finite Element Analysis, *Construction and Building Materials*, 2012; 37, 481-492.
- [9] B. Winkler, G. Hofstetter, and H. Lehar, Application of a constitutive model for concrete to the analysis of a precast segmental tunnel lining, *Int. J. Numer. Anal. Meth Geomech.* 2004; 28: 797-819.
- [10] H. Sooriyaarachchi, K. Pilakoutas, and E. Byars, Tension stiffening behavior of GFRP-reinforced concrete, *7th International Symposium on Fiber Reinforced Polymer Reinforcement for Reinforced Concrete Structures (FRPRCS-7)*, November 6-10, 2005, Kansas City, Missouri.
- [11] Peter H. Bischoff and Richard Paixao, Tension stiffening and cracking of concrete reinforced with glass fiber reinforced polymer (GFRP) bars, *Can. J. Civ. Eng.* 2004; 31: 579-588.
- [12] Yuichi Sato and Frank J. Vecchio, Tension stiffening and crack formation in reinforced concrete members with fiber-reinforced polymer sheets, *Journal of Structural Engineering* 2003; 129 (6): 717-724.
- [13] Chang-Koon Choi and Sung-Hoon Cheung, Tension stiffening model for planar reinforced concrete members, *Computers & Structures* 1994; 59(1): 179-190.
- [14] Abdelhafid Bouzaiene and Bruno Massicotte, Hypoelastic tridimensional model for nonproportional loading of plain concrete, *Journal of Engineering Mechanics*; 1997: 123(11): 1111-1119.
- [15] EN 1992-1-1. Eurocode 2 - Design of concrete structures, Part 1.1, General rules and rules for buildings. CEN; 2003.